

Communication

Absorption Properties of Simply Fabricated All-Metal Mushroom Plasmonic Metamaterials Incorporating Tube-Shaped Posts for Multi-Color Uncooled Infrared Image Sensor Applications

Shinpei Ogawa ^{1,*}, Daisuke Fujisawa ¹, Hisatoshi Hata ¹ and Masafumi Kimata ²

¹ Advanced Technology R&D Center, Mitsubishi Electric Corporation, 8-1-1 Tsukaguchi-Honmachi, Amagasaki, Hyogo 661-8661, Japan; Fujisawa.Daisuke@bc.MitsubishiElectric.co.jp (D.F.); Hata.Hisatoshi@cb.MitsubishiElectric.co.jp (H.H.)

² College of Science and Engineering, Ritsumeikan University, 1-1-1 Noji-higashi, Kusatsu, Shiga 525-8577, Japan; kimata@se.ritsumei.ac.jp

* Correspondence: Ogawa.Shimpei@eb.MitsubishiElectric.co.jp; Tel.: +81-664-977-533

Received: 4 February 2016; Accepted: 8 March 2016; Published: 11 March 2016

Abstract: Wavelength-selective infrared (IR) absorbers have attracted considerable interest due to their potential for a wide range of applications. In particular, they can be employed as advanced uncooled IR sensors that identify objects through their radiation spectra. Herein, we propose a mushroom plasmonic metamaterial absorber incorporating tube-shaped metal posts (MPMAT) for use in the long-wavelength IR (LWIR) region. The MPMAT design consists of a periodic array of thin metal micropatches connected to a thin metal plate via tube-shaped metal posts. Both the micropatches and posts can be constructed simultaneously as a result of the tube-shaped structure of the metal post structure; thus, the fabrication procedure is both simple and low cost. The absorption properties of these MPMATs were assessed both theoretically and experimentally, and the results of both investigations demonstrated that these devices exhibit suitable levels of LWIR absorption regardless of the specific tube-shaped structures employed. It was also found to be possible to tune the absorption wavelength by varying the micropatch width and the inner diameter of the tube-shaped metal posts, and to obtain absorbance values of over 90%. Focal plane array structures based on such MPMATs could potentially serve as high-performance, low-cost, multi-spectral uncooled IR image sensors.

Keywords: metamaterials; plasmonics; infrared sensors; image sensors

1. Introduction

In recent years, there has been remarkable progress in electromagnetic wave (EW) absorber technology as a result of research into plasmonics [1,2] and metamaterials [3–5]. Plasmonic metamaterial absorbers are structurally scalable, which enables a wide range of applications at various wavelengths, including solar cells in the visible range [6], biological sensors in the near infrared (IR) [7] and middle IR [8], and thermal sensors in the IR [9–12] and terahertz ranges [13,14], as well as EW shielding [15] and wireless microwave transfer [16]. Wavelength-selective IR absorbers show significant promise as advanced uncooled IR sensors since they allow the identification of objects through their radiation spectra [17], and many applications of these devices are anticipated, such as in gas analysis, fire detection, multi-color imaging [18], and hazardous materials recognition [19]. Metal-insulator-metal (MIM)-type absorbers [20,21] are important candidates for wavelength-selective uncooled IR sensors due to their small thermal mass and size. However, the presence of insulating layers, including SiO₂, Al₂O₃, and SiN, can cause spurious peaks due to intrinsic absorption [9], which

prevents these absorbers from operating at long IR wavelengths in the vicinity of $10\ \mu\text{m}$ [22]. This is an important wavelength region for the observation of living beings as well as for the sensing of gaseous compounds such as ethanol.

Recently, we reported the feasibility of mushroom plasmonic metamaterial absorbers (MPMAs) having all-metal [23,24] or silicon (Si) post [25] structures without an insulating layer as a means of addressing this issue. MPMAs consist of periodic micropatches connected to a bottom plate by posts, forming an array of mushroom-shaped antennae [26,27]. MPMAs with Si posts are consistent with complementary metal oxide semiconductor (CMOS) technology and have demonstrated sufficient wavelength-selective absorption upon varying the micropatch size. However, the fabrication of MPMAs with Si posts requires precise control over the post width in order to suppress the resonance mode in the Si posts and maintain a single mode of the localized plasmonic resonance at the micropatch [25]. On the other hand, there are no resonant modes in the metal posts, which enables single-mode operation. The construction of these mushroom-shaped structures normally requires a complicated stepwise fabrication procedure that produces the metal posts and the micropatches separately [24], and this complexity causes structural fluctuations, which degenerate the absorption properties and restrict the practical applications of MPMAs. In the present paper, we report the design and fabrication of MPMAs with tube-shaped metal posts (MPMATs) as a means of addressing this problem, and also the results of a characterization of these devices.

2. Absorber Design

Figure 1a presents a schematic of the proposed MPMAT structure. In this design, square micropatch antennae are connected to the bottom plate by tube-shaped metal posts. This tubular shape is the key to obtaining a simple fabrication procedure, as will be discussed in the fabrication section. All of the components are made from aluminum (Al) in order to reduce the overall cost, although gold, silver, or copper can also be used. Figure 1b shows a cross-sectional schematic of the MPMAT and defines the structural parameters. The period, width, and thickness of the micropatches, the inner diameter, width and height of the tube-shaped metal posts, and the thickness of the bottom plate are denoted p , w_m , t_m , w_h , w_p , h , and t_b , respectively. Here, w_p is defined as the sum of w_h and the Al sidewall thickness of 100 nm, based on a consideration of the fabrication method.

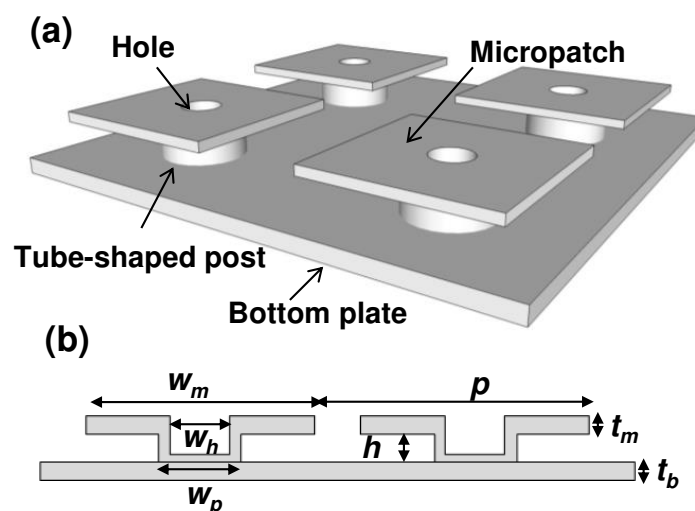


Figure 1. (a) Schematic diagram and (b) cross-sectional view of proposed mushroom plasmonic metamaterial absorber with tube-shaped metal post (MPMAT).

The absorption properties of the MPMAT were quantitatively assessed using rigorous coupled wave analysis (RCWA), fixing the values of p , t_m , h , and t_b at $6.0\ \mu\text{m}$, $100\ \text{nm}$, $200\ \text{nm}$, and $100\ \text{nm}$,

respectively. Initially, the absorption was calculated while varying w_m , with w_h held constant at 1.3 μm . Figure 2a summarizes the calculated absorbance results. These data indicate that the absorption wavelength can be controlled by varying the micropatch width, and the absorption wavelength can be longer than the micropatch period, which can lead to smaller pixel size compared with two-dimensional plasmonic absorbers [10,11]. It is evident that this device exhibits wavelength-selective absorption in the long-wavelength infrared (LWIR) region due to the lack of an insulator layer. Absorption at lower wavelengths such as in the middle-wavelength IR region can also be realized by reducing the micropatch width and the period. These properties could allow for small pixel sizes in uncooled IR sensors operating in a wideband wavelength region. Subsequently, the effect of varying the key parameter w_h on the MPMAT performance was investigated. In these trials, the value of w_m was fixed at 4.5 μm , and w_h was varied from 0.5 to 1.5 μm , representing the range possible using practical fabrication techniques assuming that the tube-shaped posts are formed by conventional photolithography. Figure 2b shows the calculated absorption properties at a normal incidence angle for various w_h . These results demonstrate that strong single-wavelength-selective absorbance of over 90% is obtained regardless of the inner diameter of the tube-shaped holes in the posts. The absorption wavelength is shifted to shorter values as the inner diameter of the tube-shaped posts is increased. This result indicates that the plasmon resonance wavelength is decreased by the presence of the holes in the micropatches.

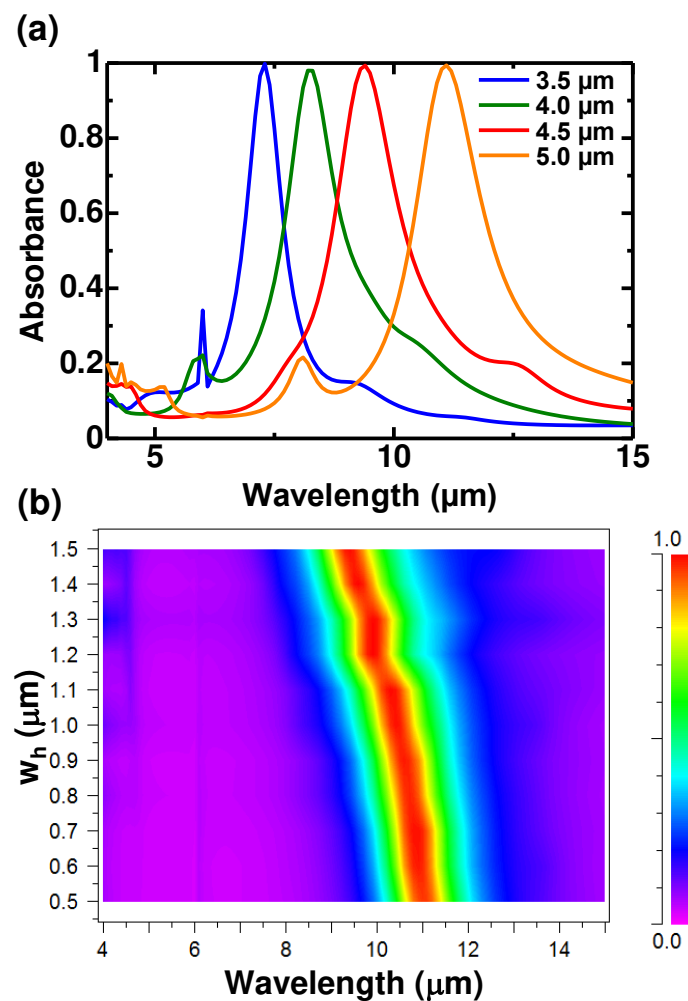


Figure 2. Calculated absorbance as a function of wavelength for various (a) micropatch widths (w_m) and (b) inner diameters of tube-shaped posts (w_h). In panel (a) w_h is fixed at 1.3 μm and in panel (b) w_m is fixed at 4.5 μm . The color-map defines the absorbance scale.

3. Fabrication

Figure 3 summarizes the sample fabrication procedure. The bottom plate is formed by sputtering a 100-nm-thick Al layer onto a Si substrate, as shown in Figure 3a. The value of t_b must be at least twice the skin depth at IR wavelengths, so a t_b of 100 nm is sufficient to prevent the penetration of incident light in this device. A 200-nm-thick Si layer is then deposited to form a sacrificial layer, and the holes for the posts are patterned using photolithography and reactive ion etching (RIE) (Figure 3b). Subsequently, a 100-nm-thick Al layer is sputtered to form the posts and to provide the micropatch material; the thickness of this layer determines the value of w_p , which is equal to the sum of w_h and the Al sidewall thickness of 100 nm. The upper Al layer is then patterned to form a periodic array of micropatches using photolithography and wet etching techniques (Figure 3c). Finally, the sacrificial Si layer is removed by XeF_2 etching to provide the complete MPMAT, as illustrated in Figure 3d. The tube-shaped post structures enable both the metal posts and the micropatches to be constructed simultaneously, thus reducing the complexity of the fabrication procedure. A slight change in w_h does not lead to diminution of the absorbance, as shown in Figure 2b, resulting in a structurally robust fabrication process. Therefore, MPMATs having tube-shaped posts are good candidates for commercially viable devices such as low-cost, high-performance, wavelength-selective uncooled IR sensors.

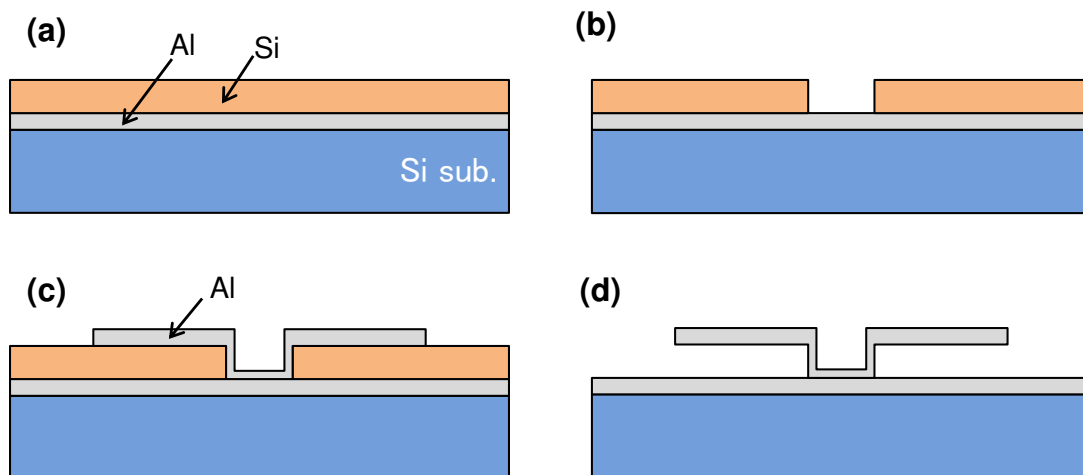


Figure 3. Procedure for fabricating the MPMATs: (a) a sacrificial Si layer is formed on a sputtered Al layer over a Si substrate; (b) holes are patterned on the Si layer by reactive ion etching (RIE); (c) an upper Al layer is added by sputtering and is patterned to form the upper micropatches; and (d) the sacrificial layer is removed by XeF_2 to complete the MPMAT.

Figure 4a–c show top, oblique, and magnified cross-sectional scanning electron microscopy (SEM) images of the newly developed MPMAT, respectively. All of our micropatches were successfully fabricated without bending or sticking. In these devices, the value of w_h can be controlled simply by varying the illumination power applied during the photolithography process. These images demonstrate that a uniform gap size of 200 nm was achieved between the micropatches and the bottom plate despite the presence of the tube-shaped post structures, providing strong plasmonic resonance. This fabrication procedure is also compatible with CMOS technology.

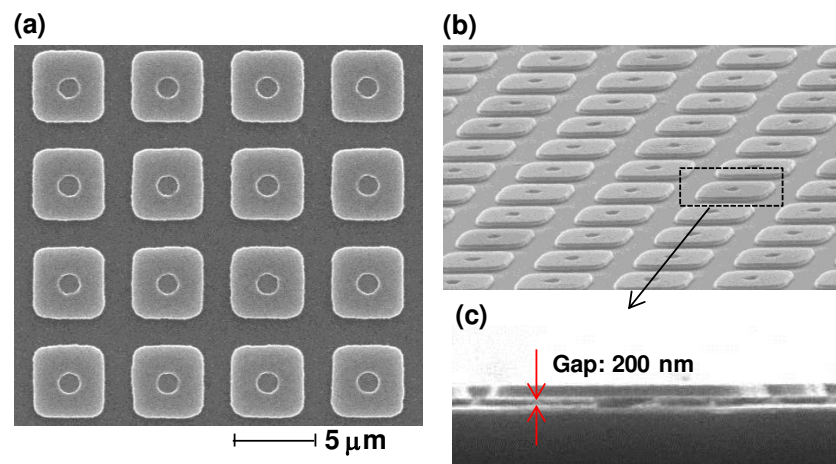


Figure 4. SEM images of an MPMAT: (a) top; (b) oblique and (c) magnified cross-sectional views of the periodic structures.

4. Measurement and Discussion

In the present study, we prepared devices operating primarily in the vicinity of $10\ \mu\text{m}$, corresponding to the region applicable to the detection of gases and living beings and where MIM structures have difficulty operating [22]. In these devices, the p , t_m , h , and t_b parameters were fixed at $6.0\ \mu\text{m}$, $100\ \text{nm}$, $200\ \text{nm}$, and $100\ \text{nm}$, respectively.

The reflectance of the devices was assessed using Fourier transform infrared spectroscopy (FTIR). During these observations, the incidence angle and the reflection angle were held constant at 15° due to the mechanical restrictions of the FTIR system used. The effect of the w_m value was investigated because this parameter was expected to determine the operational wavelength of uncooled IR sensors. Figure 5a,b present the experimental reflectance spectra obtained from specimens with w_m and w_h values of 3.5 and $1.5\ \mu\text{m}$ and 4.5 and $1.3\ \mu\text{m}$ (corresponding to Figure 4a), respectively. The insets in Figure 5 also show SEM images of each sample.

The small $200\ \text{nm}$ difference in the w_h values of these devices evidently had a minimal impact on the absorption wavelength, as shown in Figure 2b, such that these spectra exhibit strong absorbance maxima at 6.3 and $9.7\ \mu\text{m}$, respectively. These reflectance maxima directly correspond to the absorption peaks of the devices because the transmittance was zero as a result of the thick lower metal plate. Intense absorbance of over 90% was achieved with both samples, demonstrating that the absorption peak wavelength primarily depends on the micropatch width and that MPMATs can successfully operate at approximately $10\ \mu\text{m}$ in a single mode. The variations in the absorption peak wavelength with changes in w_m are in good agreement with the calculated results shown in Figure 2a.

The effect of the w_h value was subsequently investigated by preparing a sample with a w_h of $0.7\ \mu\text{m}$. This lower w_h had the effect of shifting the absorption wavelength to a shorter value, as shown in Figure 2b; therefore, a w_m value of $4.3\ \mu\text{m}$ was employed in order to allow the device to operate in the vicinity of $10\ \mu\text{m}$. Figure 5c presents the resulting reflectance spectrum, in which absorption is observed at $9.7\ \mu\text{m}$ with a very high absorbance of over 95% . This result demonstrates that the effect of w_h can be compensated for by varying w_m . Furthermore, both the theoretical and experimental results demonstrate that the absorption of the MPMAT exhibits very little incidence-angle dependence up to 15° .

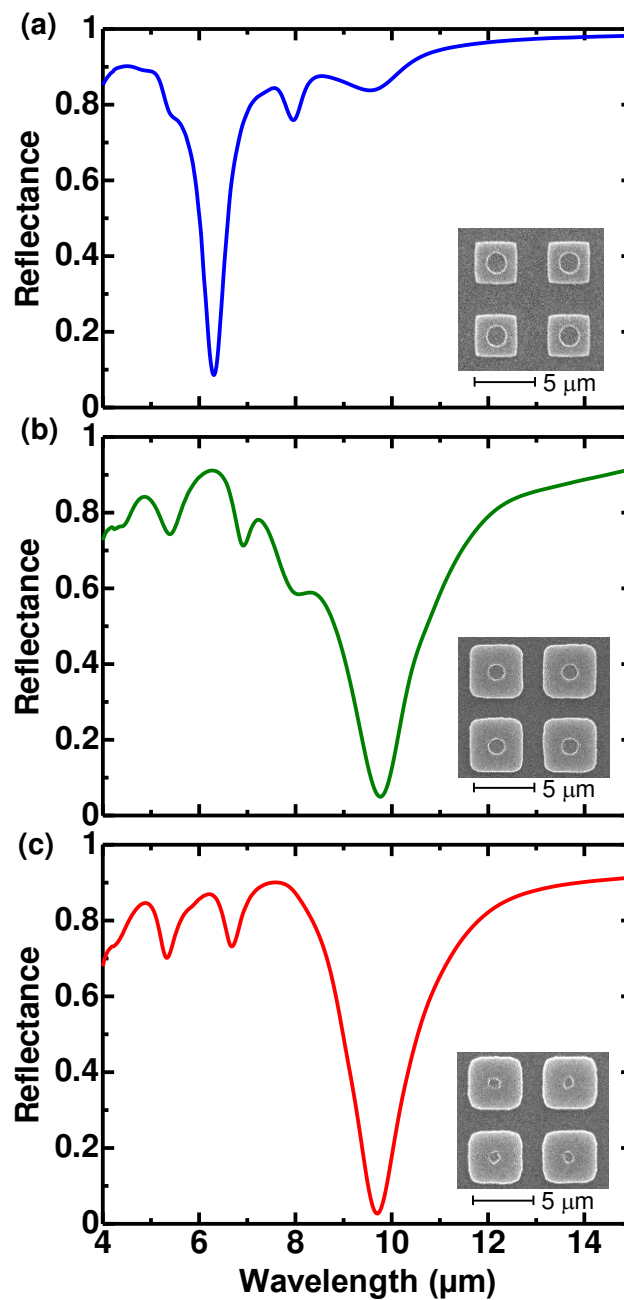


Figure 5. Experimental reflectance spectra for devices with w_m and w_h of (a) 3.5 and 1.5 μm ; (b) 4.5 and 1.3 μm ; and (c) 4.3 and 0.7 μm .

5. Conclusions

We have demonstrated a novel MPMA incorporating tube-shaped post structures that can be produced using a simple fabrication procedure and enables single-mode wavelength-selective absorption in the LWIR region. The absorption wavelength of such devices was found to be longer than the micropatch period and can be controlled by varying both the micropatch width and the inner diameter of the tube-shaped metal posts. The proposed MPMAT is a promising candidate for the construction of high-performance, wavelength-selective, uncooled IR sensors that operate in a wideband IR wavelength region and are inexpensive due to the facile production method. Potential applications of MPMATs include high-performance, wavelength-selective IR emitters

and high-performance, low-cost, multi-spectral uncooled IR image sensors based on focal plane array structures.

Acknowledgments: The authors wish to thank Koji Misaki and Mitsuharu Uetsuki for fabrication and measurement assistance, and Masashi Ueno, Takahiro Onakado, and Tetsuya Satake of the Mitsubishi Electric Corporation Advanced Technology R&D Center for their assistance during this work.

Author Contributions: S.O. conceived and designed the theoretical investigations and experiments; D.F. and H.H. fabricated the samples and performed measurements. M.K. supervised all aspects of IR sensor applications; S.O. wrote the paper.

Conflicts of Interest: The authors declare no conflict of interest.

Abbreviations

The following abbreviations are used in this manuscript:

IR	Infrared
MPMAT	Mushroom plasmonic metamaterial absorber incorporating tube-shaped metal posts
LWIR	long-wavelength IR
EW	Electromagnetic wave
MIM	Metal-insulator-metal
CMOS	Complementary metal oxide semiconductor
RCWA	Rigorous coupled wave analysis
RIE	Reactive ion etching
SEM	Scanning electron microscopy
FTIR	Fourier transform infrared spectroscopy

References

- Stanley, R. Plasmonics in the mid-infrared. *Nat. Photon.* **2012**, *6*, 409–411. [[CrossRef](#)]
- Kawata, S. Plasmonics: Future outlook. *Jpn. J. Appl. Phys.* **2013**, *52*, 010001. [[CrossRef](#)]
- Smith, D.R.; Pendry, J.B.; Wiltshire, M.C. Metamaterials and negative refractive index. *Science* **2004**, *305*, 788–792. [[CrossRef](#)] [[PubMed](#)]
- Meinzer, N.; Barnes, W.L.; Hooper, I.R. Plasmonic meta-atoms and metasurfaces. *Nat. Photon.* **2014**, *8*, 889–898. [[CrossRef](#)]
- Watts, C.M.; Liu, X.; Padilla, W.J. Metamaterial electromagnetic wave absorbers. *Adv. Mater.* **2012**, *24*, OP98–OP120. [[CrossRef](#)] [[PubMed](#)]
- Aydin, K.; Ferry, V.E.; Briggs, R.M.; Atwater, H.A. Broadband polarization-independent resonant light absorption using ultrathin plasmonic super absorbers. *Nat. Commun.* **2011**, *2*, 517. [[CrossRef](#)] [[PubMed](#)]
- Liu, N.; Mesch, M.; Weiss, T.; Hentschel, M.; Giessen, H. Infrared perfect absorber and its application as plasmonic sensor. *Nano Lett.* **2010**, *10*, 2342–2348. [[CrossRef](#)] [[PubMed](#)]
- Ishikawa, A.; Tanaka, T. Metamaterial absorbers for infrared detection of molecular self-assembled monolayers. *Sci. Rep.* **2015**, *5*, 12570. [[CrossRef](#)] [[PubMed](#)]
- Maier, T.; Brueckl, H. Multispectral microbolometers for the midinfrared. *Opt. Lett.* **2010**, *35*, 3766–3768. [[CrossRef](#)] [[PubMed](#)]
- Ogawa, S.; Okada, K.; Fukushima, N.; Kimata, M. Wavelength selective uncooled infrared sensor by plasmonics. *Appl. Phys. Lett.* **2012**, *100*, 021111. [[CrossRef](#)]
- Ogawa, S.; Komoda, J.; Masuda, K.; Kimata, M. Wavelength selective wideband uncooled infrared sensor using a two-dimensional plasmonic absorber. *Opt. Eng.* **2013**, *52*, 127104. [[CrossRef](#)]
- Ogawa, S.; Masuda, K.; Takagawa, Y.; Kimata, M. Polarization-selective uncooled infrared sensor with asymmetric two-dimensional plasmonic absorber. *Opt. Eng.* **2014**, *53*, 107110. [[CrossRef](#)]
- Alves, F.; Grbovic, D.; Karunasiri, G. Investigation of microelectromechanical systems bimaterial sensors with metamaterial absorbers for terahertz imaging. *Opt. Eng.* **2014**, *53*, 097103. [[CrossRef](#)]
- Tao, H.; Kadlec, E.A.; Strikwerda, A.C.; Fan, K.; Padilla, W.J.; Averitt, R.D.; Shaner, E.A.; Zhang, X. Microwave and terahertz wave sensing with metamaterials. *Opt. Exp.* **2011**, *19*, 21620–21626. [[CrossRef](#)] [[PubMed](#)]

15. Ding, F.; Cui, Y.; Ge, X.; Jin, Y.; He, S. Ultra-broadband microwave metamaterial absorber. *Appl. Phys. Lett.* **2012**, *100*. [[CrossRef](#)]
16. Wang, B.; Teo, K.H.; Nishino, T.; Yerazunis, W.; Barnwell, J.; Zhang, J. Experiments on wireless power transfer with metamaterials. *Appl. Phys. Lett.* **2011**, *98*, 254101. [[CrossRef](#)]
17. Talghader, J.J.; Gawarikar, A.S.; Shea, R.P. Spectral selectivity in infrared thermal detection. *Light Sci. Appl.* **2012**, *1*. [[CrossRef](#)]
18. Fujisawa, D.; Ogawa, S.; Hata, H.; Uetsuki, M.; Misaki, K.; Takagawa, Y.; kimata, M. Multi-color imaging with silicon-on-insulator diode uncooled infrared focal plane array using through-hole plasmonic metamaterial absorbers. In *MEMS*; IEEE: Estoril, Portugal, 2015; pp. 905–908.
19. Vollmer, M.; Mollmann, K.-P. *Infrared Thermal Imaging: Fundamentals, Research and Applications*; Wiley-VCH: Weinheim, Germany, 2010.
20. Liu, X.; Starr, T.; Starr, A.F.; Padilla, W.J. Infrared spatial and frequency selective metamaterial with near-unity absorbance. *Phys. Rev. Lett.* **2010**, *104*, 207403. [[CrossRef](#)] [[PubMed](#)]
21. Hao, J.; Wang, J.; Liu, X.; Padilla, W.J.; Zhou, L.; Qiu, M. High performance optical absorber based on a plasmonic metamaterial. *Appl. Phys. Lett.* **2010**, *96*, 251104. [[CrossRef](#)]
22. Chen, Y.B.; Chiu, F.C. Trapping mid-infrared rays in a lossy film with the berreman mode, epsilon near zero mode, and magnetic polaritons. *Opt. Exp.* **2013**, *21*, 20771–20785. [[CrossRef](#)] [[PubMed](#)]
23. Ogawa, S.; Fujisawa, D.; Kimata, M. Three-dimensional plasmonic metamaterial absorbers based on all-metal structures. In *SPIE*; Andresen, B.F., Fulop, G.F., Hanson, C.M., Norton, P.R., Robert, P., Eds.; SPIE: Baltimore, MD, USA, 2015; Volume 9451, p. 94511J.
24. Ogawa, S.; Fujisawa, D.; Kimata, M. Theoretical investigation of all-metal based mushroom plasmonic metamaterial absorbers at infrared wavelengths. *Opt. Eng.* **2015**, *54*, 127014. [[CrossRef](#)]
25. Ogawa, S.; Fujisawa, D.; Hata, H.; Uetsuki, M.; Misaki, K.; Kimata, M. Mushroom plasmonic metamaterial infrared absorbers. *Appl. Phys. Lett.* **2015**, *106*, 041105. [[CrossRef](#)]
26. Sievenpiper, D.; Zhang, L.; Broas, R.F.J.; Alexópolous, N.G.; Yablonovitch, E. High-impedance electromagnetic surfaces with a forbidden frequency band. *IEEE Trans. Microw. Theory Tech.* **1999**, *47*, 2059–2074. [[CrossRef](#)]
27. Kaipa, C.S.R.; Yakovlev, A.B.; Silveirinha, M.G. Characterization of negative refraction with multilayered mushroom-type metamaterials at microwaves. *J. Appl. Phys.* **2011**, *109*, 044901. [[CrossRef](#)]



© 2016 by the authors; licensee MDPI, Basel, Switzerland. This article is an open access article distributed under the terms and conditions of the Creative Commons by Attribution (CC-BY) license (<http://creativecommons.org/licenses/by/4.0/>).